

GenEDA: Unleashing Generative Reasoning on Netlist via Multimodal Encoder-Decoder Aligned Foundation Model

Wenji Fang, Wang Jing, Yao Lu, Shang Liu, Zhiyao Xie*
 Hong Kong University of Science and Technology
 *Corresponding Author

Abstract—The success of foundation AI has motivated the research of circuit foundation models, which are customized to assist the integrated circuit (IC) design process. However, existing pre-trained circuit models are typically limited to standalone encoders for predictive tasks or decoders for generative tasks. These two model types are developed independently, operate on different circuit modalities, and reside in separate latent spaces, which restricts their ability to complement each other for more advanced applications. In this work, we present GenEDA, the first framework that aligns circuit encoders with decoders within a shared latent space. GenEDA bridges the gap between graph-based circuit representations and text-based large language models (LLMs), enabling communication between their respective latent spaces. To achieve the alignment, we propose two paradigms that support both open-source trainable LLMs and commercial frozen LLMs. Built on this aligned architecture, GenEDA enables three unprecedented generative reasoning tasks over netlists, where the model reversely generates the high-level functionality from low-level netlists in different granularities. These tasks extend traditional gate-type prediction to direct generation of full-circuit functionality. Experiments demonstrate that GenEDA significantly boosts advanced LLMs’ (e.g., GPT-4o and DeepSeek-V3) performance in all tasks.

I. INTRODUCTION

The ever-increasing IC complexity and skyrocketing IC design costs are challenging traditional electronic design automation (EDA) techniques. This trend has motivated the community’s active exploration of new IC design methods, such as AI-assisted EDA techniques. Most recently, emerging *foundation AI models* have been customized and applied to IC design, named circuit foundation models [1], [2]. These pre-trained circuit foundation models target more generalized AI solutions for IC design.

Circuit foundation model: two main types. As Fig. 1 shows, existing circuit foundation models can be categorized into two main types: (a) circuit encoder for predictive tasks, and (b) circuit decoder for generative tasks. TABLE I provides a detailed comparison of these two types of works. **Circuit encoder** refers to pre-trained models that encode circuits into general embeddings (i.e., circuit representation learning). Taking these embeddings as input, various lightweight downstream models can be fine-tuned for *predictive* design tasks, such as circuit functional reasoning [3], [4], [5], [6], [7] and circuit quality prediction [8], [9], [10], [11]. **Circuit decoder** refers to pre-trained models with circuit-related *generative* capability. Built mostly on large language models (LLMs), these decoders generate text outputs, such as circuits in RTL code [12], [13], [14], verification assertions [15], [16], EDA tool scripts [17], etc.

Limitation: lack of alignment. Developed independently, circuit encoders and decoders operate on different modalities and handle circuit representations in clearly *distinct latent spaces*. Specifically: (a) Circuit encoders typically work in the circuit graph latent space. They excel at capturing circuit structural and functional properties for predictive tasks, but lack generative capabilities. (b) Circuit decoders, typically LLMs, operate in the text latent space. They are effective at generating circuit-related text (e.g., RTL code, assertions), but they rely solely on textual input and cannot fully utilize the underlying structural information of circuits. As a result,

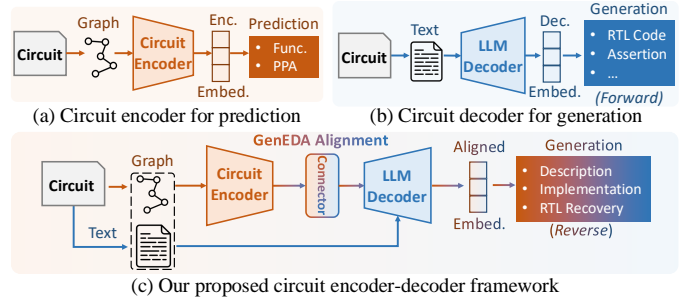


Fig. 1: (a) & (b) Two main types of existing circuit foundation models, including encoders for prediction and decoders for generation. (c) *GenEDA* proposes a general framework with alignment between circuit *encoders* and *decoders*.

these two important types are not aligned due to an inherent gap in their latent space, preventing more advanced capabilities.

GenEDA: an encoder-decoder alignment framework. In this work, we present *GenEDA*, the first framework that aligns pre-trained circuit encoders with LLM decoders. GenEDA bridges these two major types by communicating *circuit graph latent space* and *text latent space*, enabling effective information exchange. This alignment allows structural and functional insights captured by circuit encoders to directly enhance the generative capabilities of LLM decoders.

GenEDA achieves the alignment by proposing two paradigms for both open-source trainable LLMs and commercial frozen LLMs: (1) Embedding-based alignment, which fine-tunes trainable LLMs using graph-based circuit embeddings by introducing a modality *connector*, and (2) Prediction-based alignment, which augments commercial frozen LLMs by feeding them textual predictions from the encoder.

Challenging application: generative reasoning on netlist. GenEDA’s alignment framework can support unprecedentedly challenging generative applications, such as *generative reasoning on netlists*¹. Unlike RTL code, netlists are composed of a huge number of low-level, bit-blasted gates and their complex connections, offering little human-readable semantics for LLMs to understand. While prior netlist encoders [7], [23], [24], [10], [19] can extract structural and functional features into embeddings, they are limited to predictive tasks, only classifying the functionality of individual gates. GenEDA bridges this gap by aligning the encoder’s structural understanding of netlists with the decoder’s generative strengths. This encoder-decoder alignment enables generating high-level functionality directly from low-level netlist inputs, which is an unprecedentedly challenging task due to the irreversible nature of logic synthesis.

Specifically, GenEDA reasons functionalities of given netlists in a wide spectrum of granularities, with outputs including: (1) general function description, (2) circuit implementation details, and (3) fine-grained exact RTL code. These GenEDA-supported new generative

¹In netlist functionality reasoning tasks, the high-level specification and RTL code as ground-truth are unknown to the model. Models are only provided with the low-level netlist as inputs.

Arch.	Method	Input		Task			
		Format	Modality	Pred.	Gen.	Description	Direction [†]
Encoder	DeepGate [18], etc. CircuitFusion [8] MGVGA [9] NetTAG [19]	AIG	Graph	✓		function pred.	Reverse
		RTL	Graph	✓		quality pred.	Forward
		AIG	Graph & Text	✓		func./quality pred.	R/F
		Netlist	Graph & Text	✓		func./quality pred.	R/F
Decoder	RTLCoder [20], etc. HDLDebugger [21], etc. AssertLLM [15], etc DeepRTL [22]*	Spec	Text		✓	RTL gen.	
		RTL	(Image)		✓	RTL debug	Forward
		Spec	(Image)		✓	assertion gen.	
		RTL/Spec	Text		✓	RTL understand./gen.	R/F
Enc-Dec	GenEDA	Netlist	Graph&Text	✓	✓	Function gen.	Reverse

[†] Task direction is *forward* if they follow the VLSI design flow (e.g., predicting quality at the early stage, generating RTL from spec), and *reverse* if they go against it (e.g., predicting or generating function from netlist). Reverse tasks are challenging due to the design flow’s irreversible nature.

* This work [22] leverages T5, an encoder-decoder LLM. However, it targets only generative tasks, so we categorize it as a circuit decoder.

TABLE I: Comparison of GenEDA with representative categories of circuit foundation models. Existing circuit encoders mainly leverage graph structure for prediction tasks, while circuit decoders focus on semantic text for generation tasks. GenEDA bridges the gap between these two widely explored branches by aligning encoders and decoders within a shared latent space. After alignment, GenEDA supports more challenging functionality generation tasks.

netlist functional reasoning tasks are highly valuable in multiple aspects: **(1) Practical applications:** Reasoning high-level functionality from bit-blasted netlists can support critical applications such as functional verification, datapath optimization, and malicious logic detection. **(2) Unprecedented reasoning quality:** These tasks shift from traditional gate-level structural analysis to generating the overall functionality of entire circuits, including specification and RTL code, offering a significant leap in reasoning quality. **(3) Benchmarking model capability:** Our proposed tasks introduce new benchmarks for evaluating the generative capabilities and netlist understanding of foundation models. Since these tasks generate human-readable circuit information, they help enhance the interpretability of circuit models.

The contributions of this paper are summarized as follows:

- **Aligned circuit encoder-decoder framework.** We propose the first framework that aligns pre-trained circuit encoders with LLM decoders for generative tasks. It supports both trainable and frozen decoders through two alignment paradigms.
- **Generative netlist foundation model.** Building on this framework, we develop the first generative foundation model for netlists. By integrating structural and functional insights from netlist encoders, the model enhances LLM-based generation and enables reasoning over low-level, bit-blasted netlists.
- **New netlist generative reasoning tasks and benchmarks.** We introduce three novel generative functional reasoning tasks on netlists, advancing beyond prior gate-type predictions. We also release corresponding benchmarks to encourage follow-up research on these tasks.
- **Boosting SOTA LLMs’ performance.** Experimental results validate that GenEDA significantly boosts the performance of cutting-edge LLMs on all three new functional reasoning tasks after alignment with the pre-trained netlist encoder.

II. RELATED WORK

A. Method Related: Circuit Foundation Model

Recent advances in foundation AI for EDA have enabled strong generalization and generation capabilities through the *pretrain-finetune* process. As summarized in TABLE I, these *circuit foundation models* can be categorized into encoder-based and decoder-based architectures, each supporting different inputs and tasks.

Circuit encoders for prediction. Encoder-based models typically learn structured circuit representations to support predictive tasks such as reverse functional reasoning and early-stage design quality

estimation. Most methods [6], [5], [4], [25], [18], [7], [24], [10], [26] focus on AIG netlists and use graph learning to capture the circuit structure. Recent work [8], [9], [19] fuses multiple modalities (graph, text, image), but their fusion methods are limited to the encoder side, lacking alignment with LLMs for better generation. **Circuit decoders for generation.** LLM-based decoders support forward-generation tasks like RTL or assertion generation [27], [20], [28], [15], [29], debugging [21], optimization [13], [30], and knowledge querying [31], [32]. DeepRTL [22] explores bidirectional generation between RTL and specification. However, RTL is easier for LLMs due to its rich semantics, making text-only models sufficient. Additionally, existing multimodal LLMs used in these tasks focus on visual inputs, without considering circuit graph structures. **Circuit encoder-decoder alignment by GenEDA.** GenEDA bridges this gap with the first encoder-decoder alignment framework, aligning representations in a shared latent space to support advanced generation tasks.

B. Application Related: Functional Reasoning on Netlists

Functional reasoning on gate-level netlists aims to reconstruct the high-level functionality originally described in specifications or RTL. It plays a critical role in functional verification, logic optimization, datapath synthesis, and hardware security. Existing approaches primarily fall into two categories: formal methods for analyzing functionality, and machine learning methods that focus on gate-level function prediction. We detail these two categories below.

Formal analysis. Traditional methods rely on structural and functional analysis using formal techniques [33], [34], [35]. These

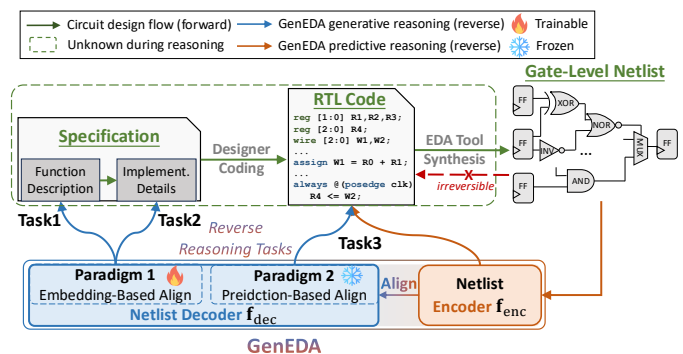


Fig. 2: Overview of GenEDA framework integrated into the standard IC design flow. GenEDA aligns the pre-trained netlist encoder with LLM decoders through two alignment paradigms, enabling challenging netlist generative functional reasoning tasks.

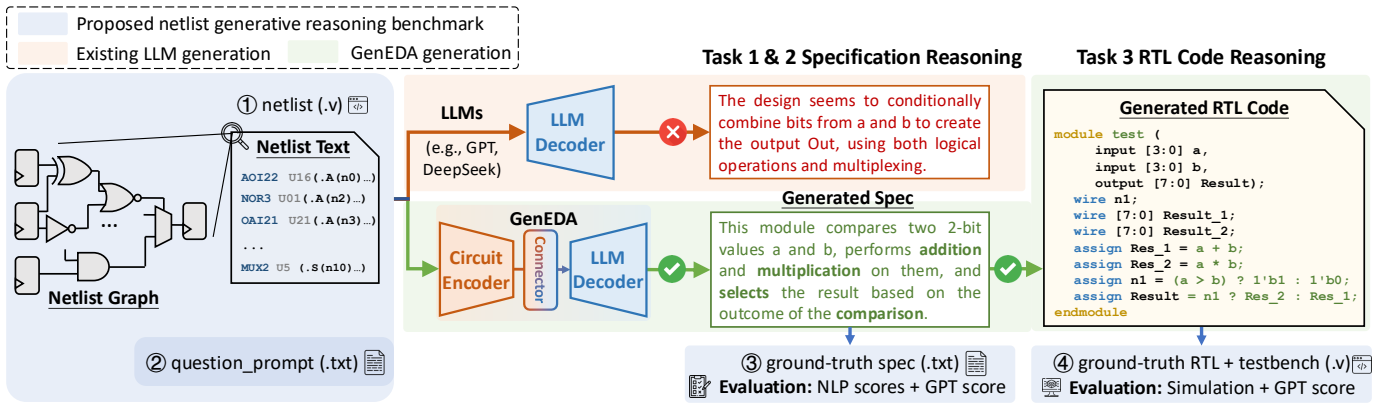


Fig. 3: Proposed netlist generative reasoning benchmark. For Tasks 1 and 2, the netlist and question prompt are processed by models for specification reasoning, and evaluated using NLP scores and GPT scores. For Task 3, the models reconstruct RTL code from the netlist, which is evaluated via simulation and GPT scores.

approaches typically extract subcircuits from the netlist and match them against components in a golden library via exhaustive formal verification. However, they are time-consuming, dependent on library completeness, and incapable of recognizing functional variants. **GNN-based prediction.** Recently, GNN-based methods [36], [37], [7], [23], [10] have been used for predictive netlist functional reasoning, focusing on gate-level function classification. While effective in identifying roles of known components, they require annotated labels and cannot generalize to unseen functionality or reason about the full circuit behavior.

Functionality generation by GenEDA. GenEDA moves beyond gate-level prediction to full-circuit generative reasoning. By aligning netlist encoders with LLM decoders, it enables direct generation of high-level specifications and RTL code from low-level gate-netlists, supporting semantics-aware understanding that goes far beyond previous prediction-based methods.

III. OVERVIEW

Fig. 2 presents the overview of our GenEDA framework, integrated into the standard digital IC design flow. GenEDA aligns the state-of-the-art post-synthesis netlist encoder NerTAG [19] f_{enc} with cutting-edge LLM-based decoders f_{dec} . It first converts the circuit netlist \mathcal{N} into embeddings via encoder f_{enc} , capturing both netlist structural and functional information. The encoder output is then provided to aligned decoders f_{dec} to support advanced generative reasoning tasks on netlists.

We propose two novel encoder-decoder alignment paradigms for both open-source trainable LLMs and commercial frozen LLMs: (1) Embedding-based alignment, where a trainable LLM decoder is instruction-tuned with encoder embeddings with a circuit modality connector. (2) Prediction-based alignment, where the encoder annotates textual gate function predictions on netlists to augment the inputs to the frozen LLM. In our experiments, we apply paradigm 1 for specification reasoning tasks (Task 1 and Task 2) and paradigm 2 for exact RTL code reasoning (Task 3).

The rest of the paper is organized as follows: In Section IV, we first provide a detailed explanation of our three novel netlist generative reasoning tasks and our contributed benchmarks. In Section V, we elaborate the two proposed encoder-decoder alignment paradigms, as well as how to tackle the three tasks. Finally, in Section VI, we demonstrate the effectiveness of GenEDA in all three generative functionality reasoning tasks in experiments.

IV. NETLIST GENERATIVE REASONING TASKS AND BECHMARKS

Fig. 3 illustrates our three novel generative reasoning tasks on netlists, along with the benchmarks developed to support them. These tasks aim to reversely generate high-level circuit functionality, including natural language specifications and exact RTL code, from low-level bit-blasted netlists. Please note that models are only provided with netlists, their corresponding specifications and RTL code serve as ground-truth and unknown to the model. Our proposed benchmarks evaluate the generative model’s ability to truly understand the functionality of netlists, setting a new direction for generative EDA tasks. We detail the three tasks below.

A. Task 1 & 2: specification reasoning from netlist.

Task and benchmark description. Tasks 1 and 2 aim to reversely generate high-level natural language specifications from gate-level netlists, as shown in Fig. 3. **Task 1 Function description generation** focuses on generating circuit functional descriptions from low-level netlists, emphasizing the overall behavior of the circuit. **Task 2 Implementation detail generation** targets the reconstruction of step-by-step signal propagation and logic behavior from the netlist, reflecting the underlying design implementation. As these are novel tasks with no prior benchmarks, we construct new datasets and benchmarks to support model training and evaluation. Specifically, we collect 400 circuit netlists with various design scales and complexities, annotated with natural language specifications as ground-truth. For each design, our proposed benchmark provides the following information in three separate files:

- **Netlist text.** Gate-level netlist in Verilog text format synthesized from RTL code. Please note that in these reverse tasks, the RTL code is unknown to the model.
- **Question prompt.** For Task 1, the prompt inquires the model to describe the interface, purpose, functionality, and constraints of the netlist. For Task 2, the prompt asks the model to explain the combinational logic, sequential behavior, and control flow.
- **Ground-truth specification text.** Since real-world RTL specifications are rarely available, we generate reference answers for these two tasks using GPT-4o prompted with RTL code and manually verify their quality through expert review.

Evaluation metrics. As there are no standard metrics for evaluating the functional similarity of specification texts, we follow prior work DeepRTL [22], which addresses the RTL-to-specification task, and adopt a combination of natural language metrics. Specifically, we use BLEU, ROUGE-1/2/L, and cosine similarity computed from

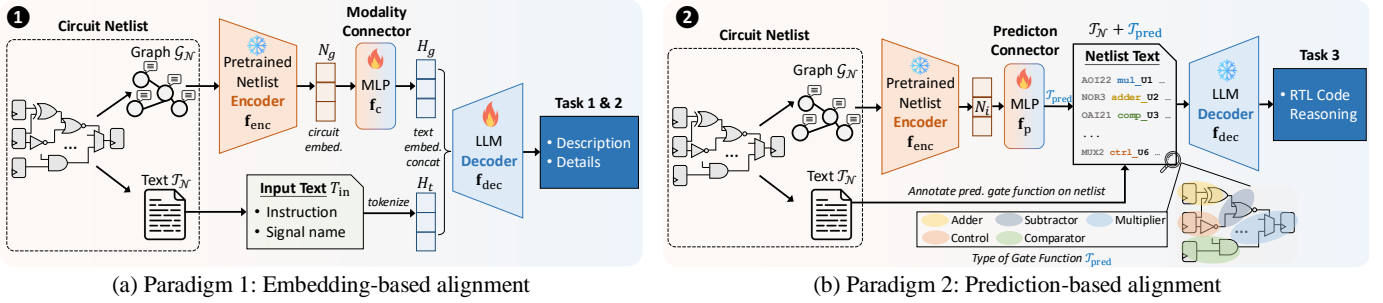


Fig. 4: Two encoder-decoder alignment paradigms in GenEDA: 1. Embedding-based alignment integrating embeddings from the netlist encoder with trainable LLM decoders, and 2. Prediction-based alignment using functional predictions from the netlist encoder as input for frozen LLM decoders.

text embeddings. Additionally, GPT-4o is employed as an automated evaluator to assess semantic similarity between generated outputs and reference specifications. The prompt templates used are provided in Section VI.

B. Task 3: arithmetic RTL code reasoning from netlist.

Task and benchmark description. **Task 3 arithmetic RTL code reasoning** targets the reverse generation of RTL code from gate-level netlists, specifically for arithmetic circuits, as shown in Fig. 3. Unlike existing *forward* RTL code generation benchmarks [38], [39], which rely on human-readable specifications as input, our *reverse* task begins with post-synthesis netlists. This makes the task significantly more challenging due to the irreversible nature of logic synthesis and the lack of high-level functional information.

We propose the first benchmark for reverse RTL code reasoning. Given the task’s complexity, we begin by focusing on arithmetic blocks. Specifically, we extend the GNN-RE gate-level arithmetic function prediction dataset [36] into a generative benchmark, incorporating golden RTL code and testbenches. For each of the 9 arithmetic designs in our benchmark, we provide:

- **Netlist text.** Gate-level netlist from GNN-RE dataset [36], originally used for gate function prediction task.
- **Question prompt.** Instructions to first infer the word-level arithmetic function, and then implement it using RTL code.
- **Ground-truth RTL code.** The original RTL design used for synthesis, which serves as the reconstruction target.
- **Testbench.** A verified testbench with predefined module name and IO ports, containing multiple input-output cases for functional validation.

Evaluation metrics. Similar to the existing forward RTL generation evaluation metrics [38], [39], we validate both syntax correctness and arithmetic functionality of the reversely generated RTL code using our provided golden testbenches. Additionally, GPT-4o is employed to assign a function similarity score, measuring how closely the generated RTL matches the ground truth. We provide detailed evaluation method implementation and prompts for obtaining GPT-score in Section VI.

V. GENEDA ENCODER-DECODER FRAMEWORK

Fig. 4 presents our proposed two paradigms for the encoder-decoder alignment, accommodating both trainable open-source LLMs and frozen commercial LLMs. Through alignment, GenEDA integrates rich netlist information captured by the encoder to enhance the generative reasoning capabilities of decoder LLMs. These two paradigms with their supported tasks are introduced in Section V-A and V-B, respectively. In our experiments, Paradigm 1 is applied to

Tasks 1 and 2 for specification reasoning, while Paradigm 2 is used for Task 3 to generate exact RTL code.

Netlist encoder and LLM decoder in GenEDA. Before discussing the alignment mechanisms, we briefly introduce the models used in GenEDA. For the encoder, we employ NetTAG [19], the state-of-the-art encoder capable of handling post-synthesis netlists, whereas most prior netlist encoders are limited to the AIG format. NetTAG introduces a text-attributed graph format for netlists and employs a multimodal architecture: it encodes the gate function via symbolic Boolean expressions by using an LLM encoder and captures global circuit structure through a graph transformer. This results in rich embeddings that encode both functional and structural information. On the decoder side, we consider both general-purpose LLMs, such as OpenAI GPT and DeepSeek, and circuit-specific LLMs like RTLCoder [20], which is fine-tuned for forward RTL code generation.

A. Paradigm 1: Embedding-Based Alignment

Paradigm 1 overview. Fig. 4 (a) shows our paradigm 1, which aligns trainable open-source LLM decoders f_{dec} with the embeddings generated by the netlist encoder f_{enc} from netlist graph (i.e., text-attributed graph) modality. The main challenge is the modality gap between the encoder-generated netlist embeddings and the text embeddings expected by the decoder, as these lie in fundamentally different latent spaces. To address this, our paradigm 1 introduces a modality connector f_c , which acts as a “circuit tokenizer”, transforming the circuit embeddings from our encoder into text-alike embeddings compatible with the LLM decoder. The connector f_c is cross-modally instruction-tuned with the LLM f_{dec} , enabling deep embedding-level alignment in the shared latent space. We describe our aligned model architecture and training method below.

Embedding alignment architecture. As shown in Fig. 4 (a), given an input netlist \mathcal{N} , we represent it in two modalities: text-attributed graph \mathcal{G}_N and netlist Verilog code \mathcal{T}_N in text format. For \mathcal{G}_N , we employ our pre-trained netlist encoder f_{enc} to process the netlist to generate the netlist graph-level embedding N_g . For the text modality \mathcal{T}_N , it is directly tokenized into language embeddings H_t and fed into the LLM decoder f_{dec} .

To align the encoded embeddings N_g with the decoder f_{dec} embedding H_t , we introduce a trainable connector MLP f_c to transform N_g into language-modal embedding tokens H_g . These converted embeddings have the same dimension as the word embedding (i.e., H_t) space in the trainable LLM decoder f_{dec} :

$$f_{dec}(H_g, H_t) \Rightarrow \text{Generative Reasoning}, \quad (1)$$

with $H_g = f_c(N_g)$ and $N_g = f_{enc}(\mathcal{G}_N)$.

Training for encoder-decoder alignment. To enhance embedding alignment, we propose cross-modal instruction tuning using task-

Human Input Example	Ground-Truth Answer Example
<pre>// 1. Instruction Please write a function description of the given circuit netlist, following this outline: (1) Interface: ... (2) Purpose: ... (3) Functionality: ... (4) Constraints: ... (Task 2 is similar) // 2. Signal name text This design is a multi-input-single- output module. The output signal is ... The input signals are: ... // 3. Graph input for circuit encoder <graph></pre>	<p>Function Description</p> <p>(1) Interface: input and output signals ... (2) Purpose: brief description of module ... (3) Functionality: brief data flow description + key states or operations ... (4) Constraints: reset and clock signals ...</p> <p>Implementation Details</p> <p>(1) Combinational logic computations: ... (2) Sequential register update function: ... (3) State machine or pipeline flow if any: ...</p>

Fig. 5: Instruction tuning data pair of alignment paradigm 1.

specific datasets (i.e., from Task 1 & 2) to achieve encoder-decoder alignment. As shown in Fig. 5, we generate a multimodal instruction-response pair for each netlist, where the input includes: (1) A task-specific instruction (e.g., request for function description or implementation details). (2) Input and output signals extracted from the netlist code. (3) The netlist graph format, with the encoder capturing the structural and functional information. The ground truth is the golden specification according to the task. This creates a unified format for multimodal instruction-following sequences. GenEDA is instruction-tuned on prediction tokens using the auto-regressive training objective, maximizing the likelihood of the target ground-truth specification text sequence y with length L , formulated as:

$$\mathcal{L}_{\text{align1}} = - \sum_{i=1}^L \log p(y_i | y_{<i}, \mathcal{G}_N) \quad (2)$$

where $y_{<i}$ represents the previously generated tokens before the current token y_i , and \mathcal{G}_N denotes the input netlist graph for the encoder.

During instruction tuning, we leverage a two-step procedure for multimodal embedding alignment:

- 1) *Pre-training for modality alignment.* In this stage, the netlist encoder \mathbf{f}_{enc} and decoder \mathbf{f}_{dec} remain frozen. Only the connector MLP \mathbf{f}_c is trained to maximize the likelihood of the generated tokens of the auto-regressive loss, as formulated in Equation (2). This step aligns the netlist embeddings H_g with the pre-trained LLM word embeddings H_t , effectively acting as a modality adapter (i.e., “netlist tokenizer”) for the LLM.
- 2) *Fine-tuning end-to-end.* In this stage, the encoder \mathbf{f}_{enc} remains frozen, while both the connector \mathbf{f}_c and the LLM decoder \mathbf{f}_{dec} are fine-tuned also with the auto-regressive loss (i.e., Equation (2)). This end-to-end training step further refines the alignment, allowing the model to perform generative tasks seamlessly across graph and text modalities.

B. Paradigm 2: Prediction-Based Alignment

Paradigm 2 overview. In addition to trainable open-source LLMs, advanced LLMs are often frozen due to commercial or computational limitations, yet they excel in reasoning and support longer input contexts. Unlike paradigm 1, which aligns coarse-grained graph-level embeddings N_g , our paradigm 2 leverages fine-grained gate-level text and frozen advanced LLMs to support the more challenging exact RTL code reasoning task. As Fig. 4 (b) shows, we align our multimodal encoder \mathbf{f}_{enc} with frozen LLM decoders \mathbf{f}_{dec} by using the encoder’s fine-grained gate functional predictions $\mathcal{T}_{\text{pred}}$ as textual inputs for LLMs. These predictions $\mathcal{T}_{\text{pred}}$ provide detailed gate-level analysis of netlist functionalities, which are then used by LLMs to summarize and generate high-level functionality. This paradigm enables seamless integration without modifying the pre-trained frozen

decoder. We introduce the details of the task and our alignment method below.

Prediction alignment architecture. To generate functional predictions $\mathcal{T}_{\text{pred}}$ with the encoder \mathbf{f}_{enc} , we fine-tune our pre-trained encoder to enable gate functionality identification with the task proposed in [36]. This task involves classifying gates into five high-level function types defined in their arithmetic RTL code: adder, multiplier, comparator, subtractor, and controller. During fine-tuning, the encoder \mathbf{f}_{enc} remains frozen, and only the additional function predictor MLP \mathbf{f}_p is trained for gate-type classification using cross-entropy loss, as formulated below.

$$\mathcal{L}_{\text{align2_pred}} = - \sum_i y_i \log(\mathbf{f}_p(N_i)), \quad (3)$$

where y_i represents the ground-truth function type label for the netlist gate i , and N_i are the encoder-generated embeddings for this gate.

After fine-tuning, the encoder generates textual predictions $\mathcal{T}_{\text{pred}}$ for all gates’ functionalities. These predictions (i.e., gate functionalities) are directly annotated into its netlist Verilog code \mathcal{T}_N , which serves as input text for the frozen LLM decoder. The decoder then utilizes this fine-grained gate annotation for arithmetic RTL code generation. To illustrate this process more clearly, we present a detailed case study in Fig. 8. We formulate the process below:

$$\begin{aligned} \mathbf{f}_{\text{dec}}(\mathcal{T}_{\text{pred}} + \mathcal{T}_N) &\Rightarrow \text{Generative Reasoning,} \\ &\text{with } \mathcal{T}_{\text{pred}} = \mathbf{f}_p(\mathbf{f}_{\text{enc}}(\mathcal{G}_N)). \end{aligned} \quad (4)$$

Chain-of-Thought for RTL code reasoning. Leveraging the annotated netlist, we employ the Chain-of-Thought (CoT) technique to improve the LLM in this challenging exact RTL code reasoning. The CoT prompt decomposes reasoning tasks into two sequential steps: (1) Reason about the word-level arithmetic function description based on the given circuit netlist with gate annotations. (2) Generate RTL code to implement the identified arithmetic function, ensuring the use of word-level operations and avoiding bit-level operations.

VI. EXPERIMENTS

In this section, we first introduce the experimental setup and evaluation metrics in Section VI-A. Then, in Section VI-C, we present our results on specification context reasoning (i.e., Task 1 & 2). Then we discuss the arithmetic RTL code reasoning results (i.e., Task 3) in Section VI-D and conclude with the ablation study in Section VI-E.

A. Experimental Settings

Circuit dataset preparation. For the circuit encoder and Task 1 & 2, we collect circuit datasets from various open-source RTL code benchmarks, including ITC99 [40], OpenCores [41], Chipyard [42], and VexRiscv [43]. In Task 1 and 2, for large sequential circuits, we split them into multiple sub-circuits, following the techniques in [19]. After splitting, we collect 25k subcircuits, which are augmented by functional equivalent transformation by Yosys [44] to create a total of 50k samples. We randomly sample 400 subcircuits for testing, ensuring that no subcircuits from the same circuit are included in

TABLE II: Statistics of the netlist dataset.

	Source	# Circuits	# Tokens (avg.)	# Gates (avg.)
Task 1 & 2	ITC99 [40]	4k	15k	1025
	OpenCores [41]	55k	9k	173
	Chipyard [42]	20k	24k	2813
	VexRiscv [43]	21k	13k	901
Task 3	GNN-RE [36]	8	4k	67

TABLE III: Evaluation results on Task 1 & 2, reasoning specification text from gate-level netlists. Best results are highlighted in bold.

Model	Task 1 Functional Description Reasoning						Task 2 Implementation Detail Reasoning					
	BLEU	ROUGE-1	ROUGE-2	ROUGE-L	Emb. Sim.	GPT Score	BLEU	ROUGE-1	ROUGE-2	ROUGE-L	Emb. Sim.	GPT Score
GPT4o	5	34	10	17	0.83	0.21	5	34	10	17	0.84	0.44
DeepSeek-V3	4	31	9	17	0.82	0.19	3	34	10	17	0.83	0.42
DeepSeek-1B	0	7	1	5	0.77	0.04	0	5	1	4	0.73	0.01
DeepSeek-7B	0	8	2	6	0.77	0.06	0	5	1	4	0.74	0.02
RTLCoder-7B	0	5	1	4	0.32	0.02	0	3	1	2	0.28	0.01
GenEDA-1B	12	47	16	27	0.9	0.62	12	47	19	28	0.93	0.5
GenEDA-7B	14	49	19	28	0.91	0.62	14	50	21	30	0.94	0.51

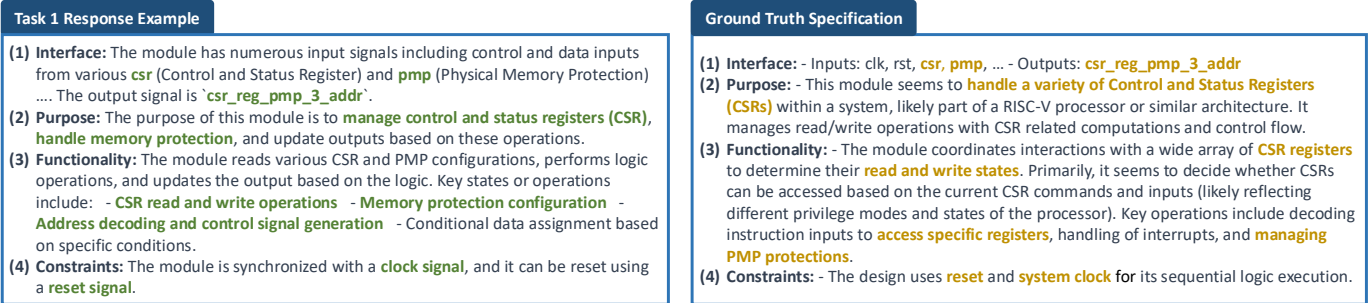


Fig. 6: Case study for Task 1. Comparison between the model-generated response and the ground truth specification for a circuit module.

the training set. Since no specification documents are available, we generate functional specifications from the RTL context using GPT-4o as the ground-truth for instruction-tuning. These generated specifications are then verified by human engineers, and those that do not contain valid functionality are excluded. For Task 3, we use the open-source arithmetic RTL code from [36]. Please note that in all tasks, only low-level netlists are provided for reverse reasoning, with high-level specifications and RTL code being unknown to models. All RTL designs are synthesized into netlists using the Synopsys Design Compiler with the NanGate 45nm technology library. We provide detailed statistics of our netlist dataset in TABLE II, including the number of circuits, the average number of text tokens, and the average number of gates.

Model and training. For the encoder model in GenEDA, we employ the state-of-the-art netlist encoder NetTAG [19] as the backbone. For the decoder LLMs in GenEDA, we fine-tune the DeepSeek-Coder [45] 1.3B and 6.7B models in the trainable embedding-based alignment (Paradigm 1), and directly leverage the commercial APIs of OpenAI GPT-4o and DeepSeek-V3 [46] as the frozen LLMs in the prediction-based alignment (Paradigm 2). The training process utilizes DeepSpeed ZeRO and LoRA techniques. In alignment paradigm 1, we adopt a three-layer MLP with dimensions 768, 2048, and 4096 to transform the netlist embedding (768 dimensions) into the LLM word embeddings (4096

dimensions). This connector can be further explored using more advanced methods, such as Q-Former and cross-attention mechanism as in [47], [48], [49]². GenEDA is instruction-tuned using LoRA on the full task-specific dataset for one epoch. In alignment paradigm 2, the function predictor MLP for encoder fine-tuning contains three layers with a hidden dimension of 256. Experiments are conducted on a server equipped with 8 NVIDIA A800 80G PCIe GPUs.

B. Benchmark Evaluation

For specification reasoning tasks (Task 1 & 2), the model-generated natural language specification is compared directly with the ground-truth specification using both natural language similarity metrics and LLM-assisted functionality evaluation metrics. Specifically, natural language similarity scores, including BLEU, ROUGE-1/2/L, are computed. These metrics assess the overlap between the generated text and the reference text by comparing n-grams. For LLM-based evaluation, we use the OpenAI text embedding model, text-embedding-ada-002, to obtain text embeddings for both the generated and reference specifications. Cosine similarity is then calculated between the embeddings to generate the embedding similarity score. Additionally, we utilize GPT-4o to directly evaluate the specifications and assign a similarity score between 0 and 1 based on how closely the generated specification matches the intended functionality of the designs. Detailed prompts for GPT-4o are provided in Fig. 7.

For RTL code reasoning (Task 3), we use Synopsys VCS to simulate the generated RTL code with the proposed testbench, validating both syntax and functional correctness. Each circuit is generated five times, and we compute the average success rate and Pass@k metrics [20]. Similar to specification reasoning, GPT-4o is also used to evaluate the functional similarity between the generated and ground-truth RTL codes, with the prompt outlined in Fig. 7.

²Complex connectors like Q-Former are typically used with frozen open-source LLMs [48], [49], while simpler connectors such as MLPs are often sufficient when the LLM is trainable [47].

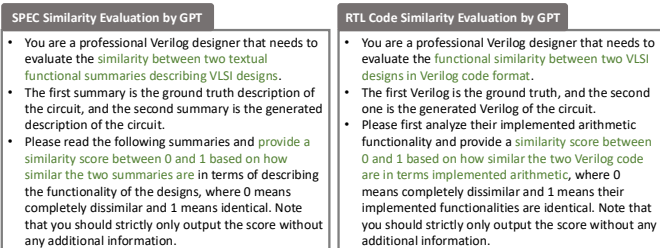


Fig. 7: Prompt used in GPT-assisted evaluation.

TABLE IV: Evaluation results on Task 3, reasoning arithmetic RTL code from gate-level netlists. Each design is generated five times per model. Best results are highlighted in bold.

Circuit	GPT-4o			GenEDA (w. GPT-4o)			DeepSeek-V3			GenEDA (w. DeepSeek-V3)		
	Syntax	GPT Score	Function	Syntax	GPT Score	Function	Syntax	GPT Score	Function	Syntax	GPT Score	Function
1	80%	0.36	0%	100%	0.52	20%	100%	0.18	0%	100%	0.85	80%
2	20%	0.32	0%	100%	0.88	80%	100%	0.55	40%	100%	0.99	100%
3	100%	0.3	60%	100%	0.28	40%	100%	0.2	0%	100%	0.74	60%
4	100%	0.66	60%	40%	0.44	20%	100%	0.95	100%	100%	1	100%
5	60%	0.18	0%	80%	0.51	0%	100%	0	0%	100%	0.98	80%
6	20%	0.2	0%	100%	0.79	60%	100%	0.28	0%	100%	0.95	100%
7	80%	0.18	0%	80%	0.54	0%	60%	0.18	0%	80%	0.91	0%
8	40%	0.28	0%	80%	0.7	0%	40%	0.49	0%	80%	0.76	0%
9	80%	0.3	0%	100%	0.56	40%	100%	0.2	0%	100%	0.78	100%
Success Rate	64%	0.31	13%	87%	0.58	29%	89%	0.34	16%	96%	0.88	69%
Pass@1	67%	/	17%	83%	/	50%	92%	/	8%	100%	/	58%
Pass@5	100%	/	22%	100%	/	67%	100%	/	22%	100%	/	78%

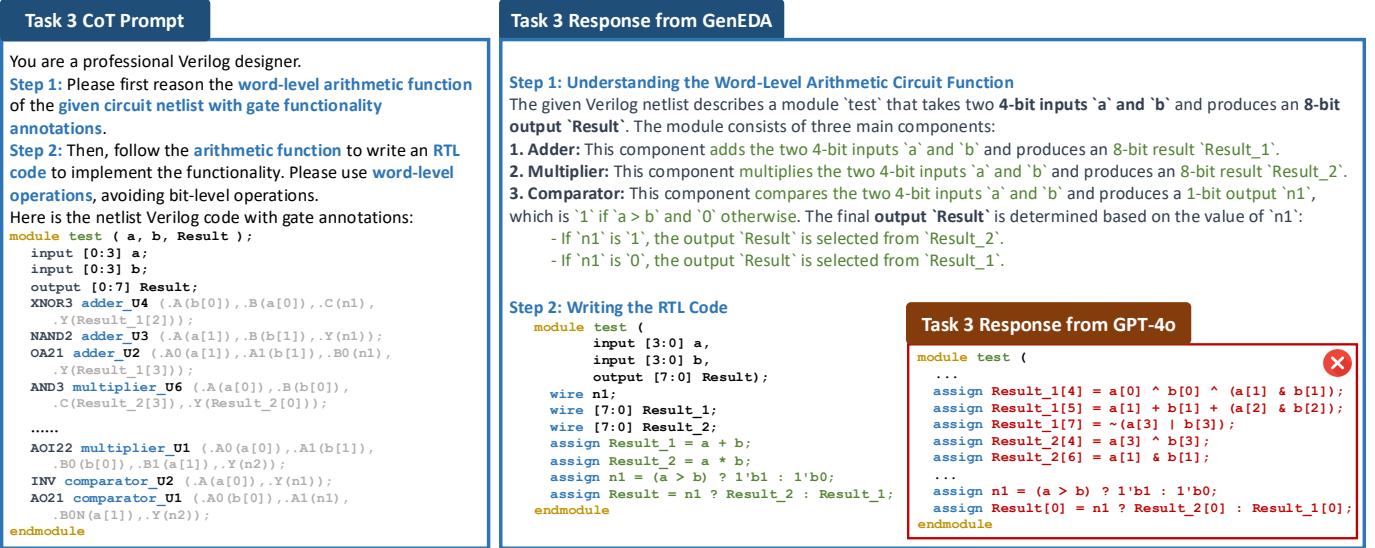


Fig. 8: Case study for Task 3. By utilizing gate function predictions from GenEDA’s encoder, the LLM in GenEDA can reason about the *word-level* arithmetic functionality of bit-blasted netlists and accurately reconstruct the corresponding RTL code (blue box). In contrast, without these predictions, LLMs (e.g., GPT-4o) generate only *bit-level* operations, leading to significantly lower reconstruction accuracy (red box).

C. Result of Specification Reasoning (Task 1 & 2)

Baseline solutions. To ensure a comprehensive comparison, we evaluate both general-purpose and circuit-adapted LLMs as baseline methods. For general-purpose LLMs, we use advanced commercial models like GPT-4o and DeepSeek-V3, as well as lightweight open-source models like DeepSeek Coder 1B and 7B. For circuit-adapted LLMs, we select RTLCoder-7B [20], a representative LLM fine-tuned for spec-to-RTL generation. These baselines take netlist text and the question prompt as input and generate the specification text.

Comparison with baselines. TABLE III presents the evaluation results for specification reasoning in Task 1 and Task 2, comparing GenEDA models with baseline models. For both tasks, after aligning with encoder embeddings through multimodal instruction tuning, our GenEDA models (1B and 7B), based on DeepSeek Coder 1B and 7B, significantly outperform all general-purpose LLMs across all textual semantic similarity metrics. Additionally, although RTLCoder [20] is fine-tuned for RTL code generation from specifications, it performs poorly on both tasks, even underperforming its base model, DeepSeek-7B. This is primarily due to the substantial differences between the tasks. Notably, for the GPT scores, which analyze the similarity between generated specification with ground truth with

GPT, GenEDA scored much higher than the baseline LLMs.

These results highlight the effectiveness of aligning circuit structural and functional information through encoders to enhance generative capabilities. Moreover, the GenEDA-7B demonstrates further improvements over the GenEDA-1B, indicating that potential gains can be achieved by employing more powerful open-sourced base models.

Natural language specification reasoning case study. We present detailed case studies for these results in Fig. 6. The figure showcases a comparison between a model-generated response and the corresponding ground truth specification for Task 1, function description generation. The model accurately generates key functionality of the specification, aligning closely with the ground truth. For example, in the functionality section, the model effectively describes how the module handles various control and status registers and memory protection configuration, which matches the ground truth’s detailed explanation of register states and operations. These results underline GenEDA’s capability to generate high-level natural language descriptions from low-level netlist inputs.

D. Result of RTL Code Reasoning (Task 3)

Baseline solutions. In this task, we choose the advanced commercial LLMs, including GPT-4o and DeepSeek-V3, as the baseline

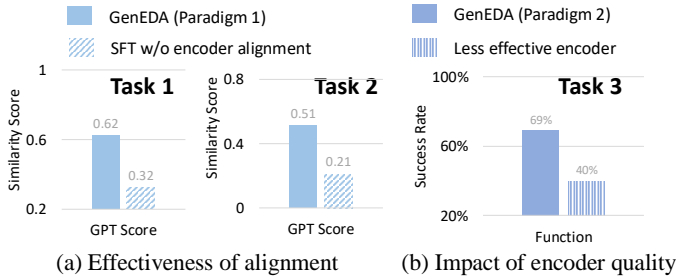


Fig. 9: Ablation study demonstrating the effectiveness of encoder-decoder alignment and the impact of encoder quality.

methods. For the open-source LLMs (e.g., DeepSeek-Coder 1B, 7B, and RTLCode), these models fail to generate high-level RTL and instead produce only gate-level netlist code.

Comparison with baselines. For netlist gate function classification, our encoder achieves a 97% accuracy rate, providing a strong foundation for our prediction-based alignment paradigm. The impact of encoder quality on alignment performance is further discussed in Section VI-E. TABLE IV evaluates Task 3: Arithmetic RTL Code Reasoning for various models. GenEDA combined with DeepSeek-V3 achieves the highest success rate with a 97% syntax pass rate, 88% GPT Score, and a 60% functional pass rate, outperforming GPT-4o, DeepSeek-V3 alone, and other combinations. Without the prediction alignment, the powerful commercial LLMs alone cannot reason the high-level word-level arithmetics to generate RTL code, and they only generate RTL code using bit-level operations. This demonstrates GenEDA’s ability to reversely reconstruct RTL code from netlists with exact functionality.

Notably, even state-of-the-art commercial LLMs like GPT-4o and DeepSeek-V3 achieve less than a 20% functional success rate on our benchmark, highlighting the difficulty of this task. In contrast, existing specification-to-RTL generation benchmarks like RTLLM [38] and VerilogEval [39] report over 60% success with off-the-shelf LLMs like GPT-4, emphasizing the challenge of reverse reconstruct high-level RTL code from low-level bit-blasted netlists.

Arithmetic RTL code reasoning case study. Fig. 8 provides an example of the reasoning process for Task 3. The Chain-of-Thought (CoT) prompt guides the model in two steps: (1) Understanding the arithmetic circuit function: The model reasons about the circuit’s gate annotations to identify components like adders, multipliers, and comparators, and determines their combined functionality. These predictions are then annotated back onto the original netlist text, which is provided to the LLM as input for further reasoning. (2) Writing the RTL code: Based on the identified functionality, the model generates RTL code using word-level operations, successfully implementing the circuit’s logic. This case study illustrates the effectiveness of GenEDA in generating correct and interpretable RTL code, bridging low-level gate details with high-level functional implementations.

E. Ablation Study

In Fig. 9, we present ablation studies to demonstrate the effectiveness of our encoder-decoder alignment and encoder quality in improving generative reasoning tasks. We conduct experiments by selectively removing the encoder alignment or using less effective encoders to assess their impact on task performance. These studies allow us to isolate and understand the contributions of different components of GenEDA to its overall performance.

Effectiveness of alignment with encoders. GenEDA alignment paradigm 1 is achieved by cross-modally fine-tuning the LLMs using

encoder embeddings. In this ablation study, we remove the encoder alignment and only perform supervised fine-tuning (SFT) of the LLMs using the same prompts and labels as in GenEDA. As shown in Fig. 9 (a), removing the encoder alignment significantly decreases model performance on Task 1 and Task 2 across all metrics. Notably, the GPT scores drop sharply from 0.62 to 0.32 on Task 1 and from 0.51 to 0.21 on Task 2, highlighting the effectiveness of embedding alignment.

Impact of encoder quality. GenEDA alignment paradigm 2 heavily relies on the accuracy of gate functionality classification from the encoder. In this ablation study, we replace the high-quality encoder NetTAG [19] with a less effective baseline, GNN-RE [36]. This results in a significant drop in classification accuracy from 97% to 83%. Consequently, the performance of reconstructed RTL code also degrades, with syntax accuracy dropping from 96% to 91% and functional accuracy from 69% to only 40%, as shown in Fig. 9 (b). This demonstrates the critical importance of using high-quality encoders in generative tasks that involve netlists.

VII. DISCUSSION

A. Extending GenEDA Alignment to Other Circuit Stages and Tasks

Beyond the netlist stage addressed in this work, GenEDA’s encoder-decoder alignment framework can be extended to various stages in the circuit design flow. At the RTL stage, even though the same RTL functionality might be present, different circuit structures can yield significantly varying PPA characteristics. By leveraging structural RTL information captured by RTL encoders, LLMs can enable structure-aware generation, potentially generating more optimized RTL code with better PPA characteristics. Additionally, at the layout stage, GenEDA can be adapted to handle cross-modal inputs, such as layout images and netlist graphs. This might enable the direct generation of macro positions on a chip by learning from image representations, thus enabling more efficient and optimized physical design generation.

B. Potential Application of Netlist Generative Reasoning

GenEDA can reason the detailed functionality from netlists, which can significantly benefit verification and optimization processes. Before loading the netlists into EDA tools, GenEDA can guide the selection of appropriate strategies for verifying or optimizing different parts of the design, such as datapaths or control logic. Additionally, it can assist in verifying the equivalence of netlists by transforming them into higher-level RTL code, making the verification process more scalable. In hardware security, GenEDA can be applied to detect malicious hardware trojans. By analyzing netlists, it can identify unexpected or unauthorized functional behaviors, helping to ensure the integrity and security of hardware systems.

VIII. CONCLUSION AND FUTURE WORK

In this paper, we present GenEDA, a framework that aligns multimodal circuit encoders and decoders for advanced generative circuit functional reasoning tasks. We align the state-of-the-art netlist encoder with both trainable and frozen LLM decoders through two alignment paradigms. Our experiments and ablation studies demonstrate the effectiveness of this approach, with GenEDA significantly enhancing the performance of state-of-the-art LLMs, showcasing the critical role of integrating both graph and text circuit modalities for complex netlist tasks. Future work will explore extending this alignment framework to other stages of the circuit design flow, such as RTL code generation and layout-stage tasks, further enhancing the capabilities of GenEDA for diverse EDA applications.

REFERENCES

- [1] L. Chen, Y. Chen, Z. Chu *et al.*, "Large circuit models: opportunities and challenges," *Science China Information Sciences*, 2024.
- [2] W. Fang, J. Wang, Y. Lu, S. Liu, Y. Wu, Y. Ma, and Z. Xie, "A survey of circuit foundation model: Foundation ai models for vlsi circuit design and eda," *arXiv preprint arXiv:2504.03711*, 2025.
- [3] W. Fang, S. Liu, H. Zhang, and Z. Xie, "A self-supervised, pre-trained, and cross-stage-aligned circuit encoder provides a foundation for various design tasks," in *ASP-DAC*, 2025.
- [4] Z. Shi, Z. Zheng, S. Khan, J. Zhang, M. Li, and Q. Xu, "Deepgate3: towards scalable circuit representation learning," *arXiv preprint arXiv:2407.11095*, 2024.
- [5] Z. Shi, H. Pan, S. Khan, M. Li, Y. Liu, J. Huang, H.-L. Zhen, M. Yuan, Z. Chu, and Q. Xu, "DeepGate2: Functionality-aware circuit representation learning," in *ICCAD*, 2023.
- [6] M. Li, S. Khan, Z. Shi, N. Wang, H. Yu, and Q. Xu, "DeepGate: Learning neural representations of logic gates," in *DAC*, 2022.
- [7] Z. Wang, C. Bai, Z. He, G. Zhang, Q. Xu, T.-Y. Ho, B. Yu, and Y. Huang, "Functionality matters in netlist representation learning," in *Design Automation Conference (DAC)*, 2022.
- [8] W. Fang, S. Liu, J. Wang, and Z. Xie, "Circuitfusion: multimodal circuit representation learning for agile chip design," in *International Conference on Learning Representations (ICLR)*, 2025.
- [9] H. Wu, H. Zheng, Y. Pu, and B. Yu, "Circuit representation learning with masked gat modeling and verilog-aig alignment," in *International Conference on Learning Representations (ICLR)*, 2025.
- [10] C. Deng, Z. Yue *et al.*, "Less is more: Hop-wise graph attention for scalable and generalizable learning on circuits," in *DAC*, 2024.
- [11] C. Xu, P. Sharma, T. Wang, and L. W. Wills, "Fast, robust and transferable prediction for hardware logic synthesis," in *IEEE/ACM International Symposium on Microarchitecture (MICRO)*, 2023.
- [12] Y. Zhang, Z. Yu *et al.*, "Mg-verilog: Multi-grained dataset towards enhanced llm-assisted verilog generation," *arXiv preprint arXiv:2407.01910*, 2024.
- [13] Z. Pei, H.-L. Zhen, M. Yuan, Y. Huang, and B. Yu, "Bettermv: Controlled verilog generation with discriminative guidance," *arXiv preprint arXiv:2402.03375*, 2024.
- [14] S. Liu, W. Fang, Y. Lu, Q. Zhang, H. Zhang, and Z. Xie, "RTLCode: Outperforming GPT-3.5 in design RTL generation with our open-source dataset and lightweight solution," *IEEE LLM-Aided Design (LAD)*, 2023.
- [15] Z. Yan, W. Fang, M. Li, M. Li, Z. Yan, S. Liu, Z. Xie, and H. Zhang, "AssertLLM: Generating and evaluating hardware verification assertions from design specifications via multi-LLMs," in *ASP-DAC*, 2025.
- [16] R. Kande, H. Pearce *et al.*, "(security) assertions by large language models," *IEEE Transactions on Information Forensics and Security (TIFS)*, 2024.
- [17] Z. He, H. Wu, X. Zhang, X. Yao, S. Zheng, H. Zheng, and B. Yu, "Chateda: A large language model powered autonomous agent for eda," in *Workshop on Machine Learning for CAD (MLCAD)*, 2023.
- [18] Z. Zheng, S. Huang, J. Zhang *et al.*, "Deepgate4: Efficient and effective representation learning for circuit design at scale," in *International Conference on Learning Representations (ICLR)*, 2025.
- [19] W. Fang, W. Li, S. Liu, Y. Lu, H. Zhang, and Z. Xie, "Nettag: A multimodal rtl-and-layout-aligned netlist foundation model via text-attributed graph," in *Design Automation Conference (DAC)*, 2025.
- [20] S. Liu, W. Fang, Y. Lu, Q. Zhang, H. Zhang, and Z. Xie, "Rtlcoder: Fully open-source and efficient llm-assisted rtl code generation technique," *IEEE TCAD*, 2024.
- [21] X. Yao, H. Li, T. H. Chan, W. Xiao, M. Yuan, Y. Huang, L. Chen, and B. Yu, "Hdldebugger: Streamlining hdl debugging with large language models," *arXiv preprint arXiv:2403.11671*, 2024.
- [22] Y. Liu, C. Xu, Y. Zhou, Z. Li, and Q. Xu, "DeepRTL: Bridging verilog understanding and generation with a unified representation model," in *International Conference on Learning Representations (ICLR)*, 2025.
- [23] N. Wu, Y. Li, C. Hao, S. Dai, C. Yu, and Y. Xie, "Gamora: Graph learning based symbolic reasoning for large-scale boolean networks," in *ACM/IEEE Design Automation Conference (DAC)*, 2023.
- [24] Z. Wang, C. Bai, Z. He, G. Zhang, Q. Xu, T.-Y. Ho, Y. Huang, and B. Yu, "Fgmn2: A powerful pre-training framework for learning the logic functionality of circuits," *IEEE Transactions on Computer-Aided Design of Integrated Circuits and Systems (TCAD)*, 2024.
- [25] S. Khan, Z. Shi, Z. Zheng, M. Li, and Q. Xu, "Deepseq2: Enhanced sequential circuit learning with disentangled representations," in *Asia and South Pacific Design Automation Conference (ASP-DAC)*, 2025.
- [26] J. Liu, J. Zhai, M. Zhao, Z. Lin, B. Yu, and C. Shi, "Polargate: Breaking the functionality representation bottleneck of and-inverter graph neural network," in *ICCAD*, 2024.
- [27] M. Liu, T.-D. Ene, R. Kirby, C. Cheng, N. Pinckney *et al.*, "Chip-NeMo: Domain-Adapted LLMs for Chip Design," *arXiv preprint arXiv:2311.00176*, 2023.
- [28] K. Chang, Y. Wang, H. Ren, M. Wang, S. Liang, Y. Han, H. Li, and X. Li, "Chippgt: How far are we from natural language hardware design," *arXiv preprint arXiv:2305.14019*, 2023.
- [29] C. Sun, C. Hahn, and C. Trippel, "Towards improving verification productivity with circuit-aware translation of natural language to systemverilog assertions," in *International Workshop on Deep Learning-aided Verification (DAV)*, 2023.
- [30] X. Yao, Y. Wang, X. Li, Y. Lian, R. Chen, L. Chen, M. Yuan, H. Xu, and B. Yu, "Rtlrewriter: Methodologies for large models aided rtl code optimization," *arXiv preprint arXiv:2409.11414*, 2024.
- [31] Y. Jiang, X. Lu, Q. Jin, Q. Sun, H. Wu, and C. Zhuo, "Fabgpt: An efficient large multimodal model for complex wafer defect knowledge queries," *arXiv preprint arXiv:2407.10810*, 2024.
- [32] H. Wu, Z. He *et al.*, "Chateda: A large language model powered autonomous agent for eda," *IEEE Transactions on Computer-Aided Design of Integrated Circuits and Systems*, 2024.
- [33] W. Li, Z. Wasson, and S. A. Seshia, "Reverse engineering circuits using behavioral pattern mining," in *2012 IEEE international symposium on hardware-oriented security and trust*. IEEE, 2012, pp. 83–88.
- [34] P. Subramanian, N. Tsiskaridze, K. Pasricha, D. Reisman, A. Susnea, and S. Malik, "Reverse engineering digital circuits using functional analysis," in *DATE*, 2013.
- [35] A. Gascón, P. Subramanian, B. Dutertre, A. Tiwari, D. Jovanović, and S. Malik, "Template-based circuit understanding," in *Formal Methods in Computer-Aided Design (FMCAD)*. IEEE, 2014, pp. 83–90.
- [36] L. Alrahis, A. Sengupta *et al.*, "Gnn-re: Graph neural networks for reverse engineering of gate-level netlists," *IEEE Transactions on Computer-Aided Design of Integrated Circuits and Systems (TCAD)*, 2021.
- [37] S. D. Chowdhury, K. Yang, and P. Nuzzo, "Reignn: State register identification using graph neural networks for circuit reverse engineering," in *ICCAD*, 2021.
- [38] Y. Lu, S. Liu, Q. Zhang, and Z. Xie, "RTLMLM: An open-source benchmark for design rtl generation with large language model," in *Asia and South Pacific Design Automation Conference (ASP-DAC)*, 2024.
- [39] M. Liu, N. Pinckney, B. Khailany, and H. Ren, "VerilogEval: Evaluating large language models for verilog code generation," *arXiv preprint arXiv:2309.07544*, 2023.
- [40] F. Corno, M. S. Reorda, and G. Squillero, "RT-level ITC'99 benchmarks and first ATPG results," *IEEE Design & Test of Computers*, 2000.
- [41] *OpenCores: The reference community for Free and Open Source gateware IP cores*, <https://opencores.org/>.
- [42] A. Amid, D. Biancolin, A. Gonzalez, D. Grubb, S. Karandikar, H. Liew, A. Magyar, H. Mao, A. Ou, N. Pemberton *et al.*, "Chippyard: Integrated design, simulation, and implementation framework for custom SoCs," *IEEE Micro*, 2020.
- [43] VexRiscv, "VexRiscv: A FPGA friendly 32 bit RISC-V CPU implementation," 2022. [Online]. Available: <https://github.com/SpinalHDL/VexRiscv>
- [44] C. Wolf, J. Glaser, and J. Kepler, "Yosys-a free verilog synthesis suite," in *Austrian Workshop on Microelectronics (Austrochip)*, 2013.
- [45] D. Guo, Q. Zhu, D. Yang, Z. Xie, K. Dong, W. Zhang, G. Chen, X. Bi, Y. Wu, Y. Li *et al.*, "Deepseek-coder: When the large language model meets programming—the rise of code intelligence," *arXiv preprint arXiv:2401.14196*, 2024.
- [46] A. Liu, B. Feng, B. Xue, B. Wang, B. Wu, C. Lu, C. Zhao, C. Deng, C. Zhang, C. Ruan *et al.*, "Deepseek-v3 technical report," *arXiv preprint arXiv:2412.19437*, 2024.
- [47] H. Liu, C. Li, Q. Wu, and Y. J. Lee, "Visual instruction tuning," *Advances in neural information processing systems*, vol. 36, 2024.
- [48] J. Li, D. Li, S. Savarese, and S. Hoi, "Blip-2: Bootstrapping language-image pre-training with frozen image encoders and large language models," in *ICML*, 2023.
- [49] J. Li, D. Li, C. Xiong, and S. Hoi, "Blip: Bootstrapping language-image pre-training for unified vision-language understanding and generation," in *International Conference on Machine Learning (ICML)*, 2022.